Common-path phase-shifting lensless holographic microscopy

Vicente Micó* and Javier García

Departamento de Óptica, Universitat de Valencia, Doctor Moliner, 50, 46100 Burjassot, Spain
**Corresponding author: vicente.mico@uv.es*

Received August 24, 2010; revised October 26, 2010; accepted October 31, 2010;
posted November 2, 2010 (Doc. ID 133628); published November 22, 2010

We present an approach capable of high-NA imaging in a lensless digital in-line holographic microscopy layout even outside the Gabor's regime. The method is based on spatial multiplexing at the sample plane, allowing a common-path interferometric architecture, where two interferometric beams are generated by a spatial light modulator (SLM) prior to illuminating the sample. The SLM allows phase-shifting interferometry by phase modulation of the SLM diffracted beam. After proper digital processing, the complex amplitude distribution of the diffracted object wavefront is recovered and numerically propagated to image the sample. Experimental results are reported that validate the proposed method. © 2010 Optical Society of America

OCIS codes: 050.5080, 070.7345, 090.1995, 100.2000, 110.0180.

Digital in-line holographic microscopy (DIHM) [1,2] supposes a modern realization of the original idea proposed by Gabor in 1949 [3], where an imaging wave caused by diffraction at the sample plane interferes with a reference wave incoming from the nondiffracted light passing through the sample and the result is recorded by an electronic imaging device (typically a CCD). When the imaging wave can be considered as a perturbation of the reference wave (weak diffraction assumption), holography rules the process and the imaging wave is recovered by using classical reconstruction holographic tools applied in the digital domain. Otherwise (strong diffraction assumption), the sample excessively blocks the reference wave and diffraction dominates the process, preventing an accurate image reconstruction. In that sense, several configurations had been proposed over the years in both classical [4–6] and digital [7–9] modes to circumvent the weak diffractive condition imposed by the Gabor regime.

Recently proposed, a spatial light modulator (SLM) placed at the Fourier plane of a modified holographic Gabor-like setup allows dc term modulation (nondiffracted light) of the illumination beam [10]. Because the complex diffracted field is retrieved using a phase-shifting procedure, the method is applicable not only to weak diffractive objects, as in the Gabor approach, but for any type of samples. However, the need to allocate the SLM between the object and the CCD limits the maximum achievable resolution. In spite of that, the resolution limit can be improved by synthetic aperture (SA) generation obtained by CCD shift at the recording plane [11]. Resolution improvement in DIHM to reach high-NA values (within the 0.45–0.7 range) can be conducted by means of immersion holography [12], digital processing tools [13], subpixel shift strategy [14], and SA generation [15].

In this Letter, we report on a novel DIHM architecture capable of high-NA imaging while extending the applicability of DIHM outside the Gabor condition. The experimental setup is depicted in Fig. 1. A collimated laser beam is directed to a reflective SLM that displays a phase-profile lens having the shortest focal length allowed by the Nyquist sampling criterion for the SLM pixel size. The SLM-reflected beam has now, for our interest, two contributions: a collimated beam incoming from the zero-order term and a convergent beam incoming from the first positive order of the SLM lens. Both beams are directed toward and focused by a high-NA condenser lens, providing two different laser spots with a given axial separation: the collimated beam is focused at the image focal point (let us call it the reference spot), while the convergent beam is focused a bit prior to that point (let us call it the image spot). Then, if the object is placed just at the image focal point of the condenser lens and a clear object region spatially coincides with the reference spot, that spot plays the role of reference point source diverging from the plane containing the object. On the other hand, the image spot acts as spherical point-divergent illumination over a wide object area. Such configuration defines a common-path interferometric digital in-line holographic setup, where the reference beam is transmitted by spatial multiplexing at the sample plane. Thus, the proposed setup is based on a digital lensless Fourier holographic architecture like [9] but uses an in-line scheme instead of off-axis mode for the reference beam insertion. For this reason, the real image term overlaps at the Fourier domain with both the zero-order and the twin image terms, and a phase-shifting strategy must be implemented to remove the unwanted terms.

The phase-shifting process is performed by adding a phase step (in the form of a linear phase factor) to the SLM phase-profile lens, allowing the recording of a set of in-line holograms with different phase delays between the reference and imaging beams and permitting the application of a conventional phase-shifting algorithm. Once the whole set of phase-shifted in-line sample holograms is stored in the computer memory (recording of the sample), the digital postprocessing schematized in Fig. 2 is conducted. Note that the images included in Fig. 2 are

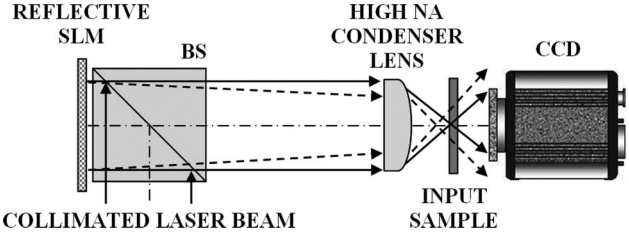

Fig. 1. Experimental setup of the proposed approach.

experimental results provided by the proposed approach, where the reference spot coincides with the transparent square (34.75 μm × 34.75 μm side) of the Groups 6 and 7 of a negative United States Air Force (USAF) resolution test. First, a conventional phase-shifting algorithm [10,11,16] recovers the complex amplitude distribution diffracted by the test. A phase-shifting process over a full test transparent area (recording of the reference) is also performed for two reasons. (1) It serves as the preliminary system calibration to precisely know the axial separation between the two (reference and image) laser spots since it is possible to numerically compute a Fresnel zone that accurately matches the one provided by the recording of the reference. (2) It can be used to minimize noise factors in the reconstruction process and improve final image quality. Continuing with our chart (Fig. 2), the second step computes the ratio between the recovered complex object information and the complex distribution incoming from the recording of the reference just to remove noise artefacts. Third, a coordinate transformation is applied to the resulting image to avoid geometric distortion when recording holograms at high NA (outside paraxial approximation) in DIHM [1,9,12,13]. Fourth, the resulting distribution is numerically propagated to focus the reference spot, and that spot and its surrounding area is blocked to improve final image quality. Fifth, the object is imaged by using digital propagation tools again. The convolution method applied to the diffraction Rayleigh–Sommerfeld integral has been used as a numerical propagation algorithm [10,11,15,16].

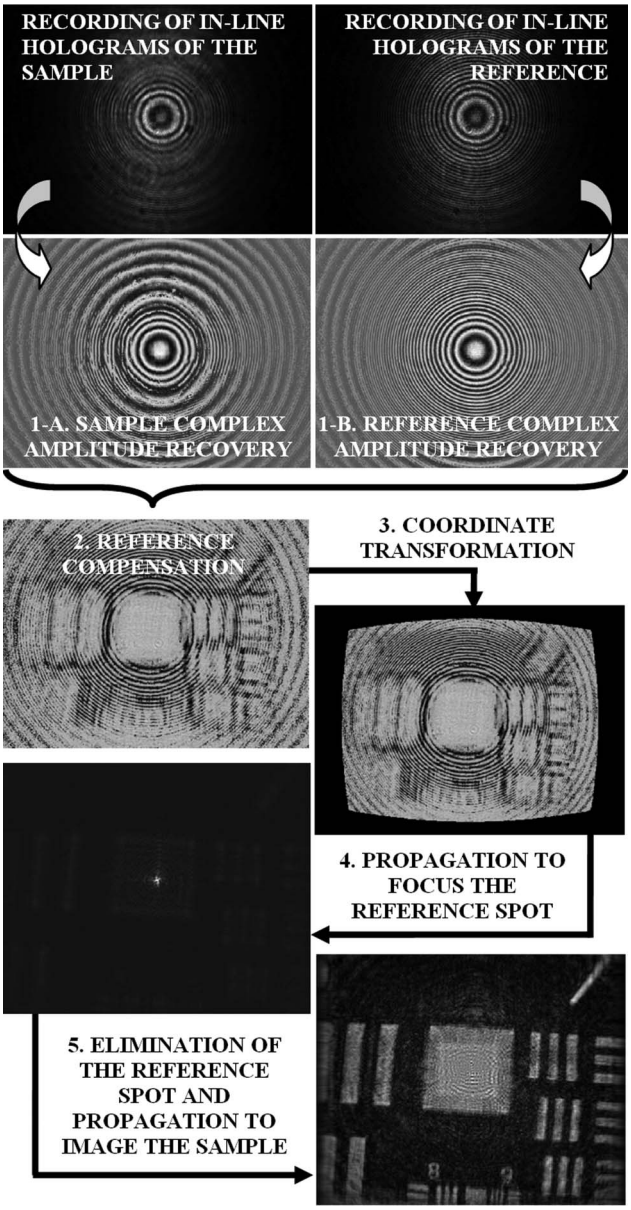

Fig. 2. Schematic chart of the digital postpropagation for the proposed common-path phase-shifting DIHM approach.

In the experimental validation, collimated illumination (532 nm laser wavelength, 50 mW optical power, 10 mm beam diameter) impinges onto a reflective SLM (Holoeye HEO 1080P, 1920 × 1080 pixels, 8 μm pixel pitch) after reflection in a nonpolarizing beam splitter (BS) cube (20 mm × 20 mm size). The SLM is connected to a computer where the phase-profile lens is mathematically modeled as $l = \exp(i2\pi(x^2 + y^2)/\lambda f)$, in which (x, y) are the discretized spatial coordinates, λ is the laser wavelength, and f is the focal length. The focal length is set to a minimum value of 1.35 m, avoiding aliasing at the SLM peripheral area. A 0.65 NA 40× commercial-grade microscope objective is used as a condenser lens and a dismantled (board level) CCD camera (Basler A312f, 582 × 782 pixels, 8.3 μm pixel size) records the images.

A set of 35 in-line holograms compose the full phase-shifting cycle. Figures 3(a) and 3(b) show one of the stored in-line holograms in the sample and reference recording cases, respectively, while the whole in-line hologram set is shown in Media 1 and Media 2, respectively. Figure 3(c) shows the Fourier transformation (FT) of Fig. 3(a) to clearly show the overlapping between the different hologram orders, while Fig. 3(d) shows the FT of the complex distribution provided by the phase-shifting process containing only the real image term. Then, the resulting distribution is digitally propagated to the reference spot plane to minimize its contribution from the final image reconstruction. Finally, numerical propagation

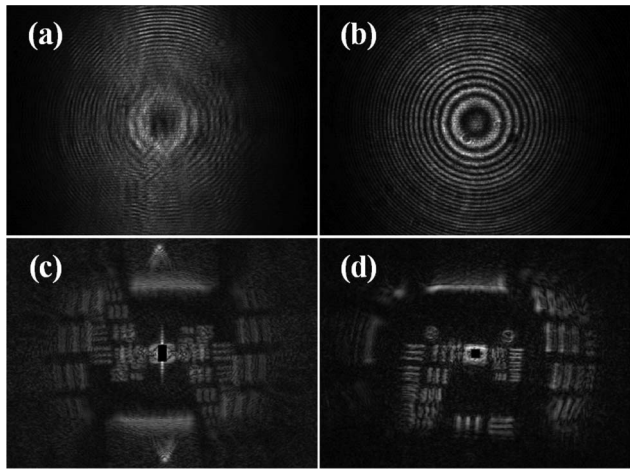

Fig. 3. In-line hologram example of (a) the USAF test (Media 1), (b) a transparent area in the test (Media 2), (c) FT of the hologram depicted in (a), and (d) FT of the resulting complex distribution provided by the phase-shifting process. Note that the dc term has been blocked down in (c) and (d) to enhance image contrast, and no coordinate transformation is applied to avoid geometrical distortion.

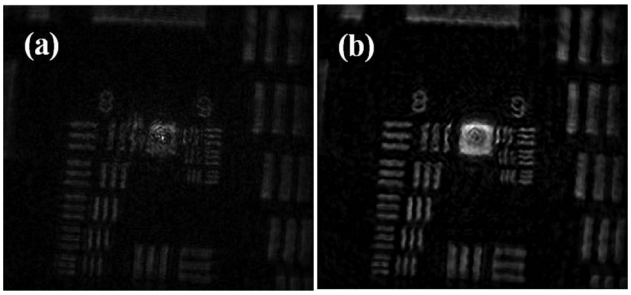

Fig. 4. Experimental results (a) without and (b) with minimizing the reference spot in the final reconstruction.

allows the final sample image. Figures 4(a) and 4(b) depict the images obtained without and with minimizing the reference spot, which is now passing through the USAF clear square (8.75 μm × 8.75 μm side) of Groups 8 and 9. We want to stress that imaging is extremely degraded in DIHM when using non-Gabor-like objects (mostly black background) [10]; hence, the images included in Fig. 4 are self sufficient and support the proposed method.

By propagating the resulting sample distribution to its best imaging plane, we precisely obtain the distance between the CCD and sample planes (z_1). The same procedure is applied for the reference case to determine the axial separation between the two laser spots (z_2). In our setup, such distances are $z_1 = 5.77$ mm and $z_2 = 0.25$ mm, and the layout magnification factor ($M = (z_1 + z_2)/z_2$) is $M = 24$, allowing that a 1 μm pitch object detail will be properly sampled by the CCD pixel size. Nevertheless, the M value can be increased by decreasing z_2 or, what is the same, by increasing the SLM lens focal length. This could be the case of using a higher NA condenser lens, where z_1 must be decreased to adapt the NA defined by the CCD to the condenser lens NA. In that sense, the resolution provided by the proposed method can be as high as that one defined by the condenser lens NA, and the z_2 distance can be properly matched to provide the correct M value. In our case, the number and size of the CCD pixels and the z_1 distance define an NA of around 0.40 for the shorter and 0.50 for the larger CCD directions and, consequently, 1.33 and 1.06 μm resolution limits, respectively. Those values are enough to resolve the smallest details of the USAF test (1.55 μm pitch, Group 9-Element 3). In addition, the object field of view (FOV) provided by the proposed method is 120 μm, approximately, as one can see from the final reconstructed image width. According with theoretical specifications, this value is comparable to that one provided by a 0.55 NA 50× Mitutoyo infinity-corrected long working distance lens when using a 1/2 in. sensor size. Finally, the proposed method can be configured for using nonsophisticated high-NA (around 0.8 NA) condenser lenses, such as, for instance, glass Blu-ray units or aspheric plastic moulded lenses, since the condenser lens needs to be stigmatic only for a single focusing spot not for a wide FOV.

In summary, we have reported on a new DIHM configuration based on a common-path architecture that allows complex amplitude sample information recovery by phase-shifting interferometry. Proof of principle validation of the method has been experimentally demonstrated using a negative USAF resolution test, and analysis of the main system parameters (M value, NA, resolution limits, and FOV) has been presented showing an open layout that can be designed depending on imaging requirements. The need for a transparent region in the object FOV is not a restrictive constraint because a very small area (comparable to the reference spot size) is needed in comparison with the FOV provided by the method. Moreover, it is possible to design a special chamber containing a clear region acting as a pinhole and place this around the sample, enabling the application of the proposed method to biomedical specimens outside the weak diffractive condition imposed by the classical Gabor approach.

Part of this work has been supported through grants from the Spanish Ministerio de Educación y Ciencia under the project FIS2010-16646.

References

1. W. Xu, M. H. Jericho, I. A. Meinertzhagen, and H. J. Kreuzer, Proc. Natl. Acad. Sci. USA **98**, 11301 (2001).
2. L. Repetto, E. Piano, and C. Pontiggia, Opt. Lett. **29**, 1132 (2004).
3. D. Gabor, Nature **161**, 777 (1948).
4. E. N. Leith and J. Upatnieks, J. Opt. Soc. Am. **53**, 1377 (1963).
5. D. Gabor and W. P. Goss, J. Opt. Soc. Am. **56**, 849 (1966).
6. G. W. Stroke, Appl. Phys. Lett. **6**, 201 (1965).
7. U. Schnars, J. Opt. Soc. Am. A **11**, 2011 (1994).
8. I. Yamaguchi and T. Zhang, Opt. Lett. **22**, 1268 (1997).
9. Y. Takaki and H. Ohzu, Appl. Opt. **38**, 2204 (1999).
10. V. Micó, J. García, Z. Zalevsky, and B. Javidi, Opt. Lett. **34**, 1492 (2009).
11. V. Micó, L. Granero, Z. Zalevsky, and J. García, J. Opt. A **11**, 125408 (2009).
12. J. Garcia-Sucerquia, W. Xu, M. H. Jericho, and H. J. Kreuzer, Opt. Lett. **31**, 1211 (2006).
13. M. Kanka, R. Riesenberg, and H. J. Kreuzer, Opt. Lett. **34**, 1162 (2009).
14. W. Bishara, T. W. Su, A. F. Coskun, and A. Ozcan, Opt. Express **18**, 11181 (2010).
15. V. Micó and Z. Zalevsky, J Biomed. Opt. **15**, 046027 (2010).
16. T. Kreis, *Handbook of Holographic Interferometry: Optical and Digital Methods* (Wiley-VCH, 2005).